

In adsorption on Si(112) and its impact on Ge growth

M. Speckmann
Th. Schmidt
J. I. Flege
J. Falta

The change of the Si(112) surface morphology and structure induced by In adsorption, as well as the impact of In preadsorption on the growth kinetics and island morphology in Ge/Si(112) epitaxy, has been investigated by means of low-energy electron microscopy and diffraction. The intrinsically faceted Si(112) surface is smoothed upon In saturation. In contrast to a previously reported (7×1) reconstruction (reported in a recent work of Gai et al.), we observe a $[(3+x) \times 1]$ superstructure, with $x \approx 1/2$. This is attributed to the coexistence of (3×1) and (4×1) building blocks with In vacancies. The presence of such vacancy rows is confirmed by the saturation of the $[(3+x) \times 1]$ structure at about 0.8 monolayers. Ge growth on In-saturated Si(112) leads to the formation of 3-D islands, the morphology of which depends on the growth temperature. At 450°C, isotropic and dashlike islands are observed, whereas at 500°C, larger islands with a triangular outline are found. The orientation of the side facets of these triangular islands have been identified to be (111), (013), and (103). The dependence of the island density on the growth temperature indicates an enhanced Ge surface diffusion, as compared with growth on bare Si(112).

Introduction

The adsorption of group-III metals on Si and Ge surfaces has been intensively studied for (001) and (111) surfaces. The technological potential for this class of material systems is mainly based on the surface passivation that is achieved by the adsorption of the trivalent metals on the group-IV semiconductors. Such a passivation can play an important role in surface functionalization, for example, for inorganic/organic material interfaces, where the interaction between the inorganic substrate and organic adlayers is modified by the group-III substrate termination. Another field of application is Ge/Si heteroepitaxy, where the growth mode has been shown to be drastically influenced if the surface is passivated prior to growth [1–9]. As Ge/Si growth is usually performed at elevated temperatures that provide sufficient activation energy for site-exchange processes [10], and since it is energetically favorable to keep the surface passivated, the group-III metals will, in general, segregate to the surface during Ge/Si growth [5, 11].

In contrast to low-index surfaces like Si(111) and Si(001), vicinal surface orientations like Si(112) or Si(113) provide less symmetry, which can be exploited for the growth of

anisotropic nanostructures such as quantum wires. For instance, Ge nanowires can be grown on bare Si(113) in a narrow temperature window [12, 13]. In the case of Ga preadsorption on Si(113), the surface is completely decomposed into (112) and (115) facets, which can be employed to increase the density and to change the orientation of the Ge wires [14]. Hence, for a better understanding of the influence of metal preadsorption on subsequent Ge growth, the investigation of the adsorbate-induced change in substrate surface reconstruction and morphology is an important issue [15, 16]. For indium on silicon, many studies can be found for (111) and (001) surface orientations. In the case of In/Si(112), the only report is by Gai et al. [17], who found that the intrinsically faceted [18, 19] Si(112) surface is smoothed upon In adsorption and exhibits a (7×1) reconstruction. In this paper, we revisit the In/Si(112) surface structure and show that the surface reconstruction does not have a (7×1) but rather a $[(3+x) \times 1]$ periodicity, with x close to 1/2.

The impact of group-III metals on Ge growth on Si(112) has been already studied for Ga. Ga adsorption also leads to smoothing of the Si(112) surface [20, 21], and a $[(5+x) \times 1]$ reconstruction is found [22]. Subsequent Ge deposition on Ga-terminated Si(112) enables the growth

Digital Object Identifier: 10.1147/JRD.2011.2158763

© Copyright 2011 by International Business Machines Corporation. Copying in printed form for private use is permitted without payment of royalty provided that (1) each reproduction is done without alteration and (2) the Journal reference and IBM copyright notice are included on the first page. The title and abstract, but no other portions, of this paper may be copied by any means or distributed royalty free without further permission by computer-based and other information-service systems. Permission to republish any other portion of this paper must be obtained from the Editor.

0018-8646/11/\$5.00 © 2011 IBM

of wirelike Ge islands, whereas rather isotropic Ge islands are found for growth on bare Si(112) [22]. For In, however, no reports on the influence on Ge growth on Si(112) are found in the literature. Therefore, this paper addresses this issue and reveals the In-induced change in Ge growth kinetics and island morphology.

Experimental details

The low-energy electron microscopy (LEEM) and diffraction (LEED) measurements were performed at the LEEM/PEEM end station [23] of beamline U5UA at the National Synchrotron Light Source (NSLS), Brookhaven National Laboratory. The experiments were performed under ultrahigh-vacuum (UHV) conditions with a base pressure in the low 10^{-10} mbar range. The microscope is a LEEM III by Elmitec, which is equipped with an electron energy analyzer for additional use as an x-ray photoemission electron microscope.

The silicon samples were cut from a Si(112) wafer with a miscut of less than 0.1° . After transfer into the UHV system, the samples were degassed at around 600°C for at least 12 hours to remove impurities from the surface and the sample holder. The native oxide layer was removed by several short flash heating cycles up to $1,200^\circ\text{C}$. After this procedure, a clear diffraction pattern was observed in LEED, and no contamination was obvious from LEEM images. Heating was performed by electron bombardment from the backside of the samples. The temperature was monitored with a thermocouple attached to the sample holder and with an infrared pyrometer operating at wavelengths below $1.1\ \mu\text{m}$.

Subsequently, indium was adsorbed on the clean Si(112) surface at a deposition temperature of 500°C , until In saturation coverage was reached, i.e., until the LEED pattern did not change anymore. Ge was grown onto In-saturated Si(112) at deposition temperatures between 450°C and 500°C . During Ge growth, In was co-deposited, i.e., the In flux was kept on, in order to compensate for In desorption. For the deposition of both materials, an electron beam evaporator (Omicron Triple EFM) was employed. The evaporator fluxes were calibrated in separate experiments on Si(111) substrates, via the well-known $(\sqrt{3} \times \sqrt{3})\text{-R}30^\circ\text{-In}$ and $(4 \times 1)\text{-In}$ reconstructions and the transition of the (7×7) to the $(5 \times 5)\text{-Ge}$ structure on the Si(111) surface, respectively. The $(\sqrt{3} \times \sqrt{3})\text{-R}30^\circ$ reconstruction is completely evolved at a coverage of $1/3\ \text{ML}_{111}$ [24–26], whereas the (4×1) reconstruction is completely evolved at a coverage of $1\ \text{ML}_{111}$ [25, 27, 28], where $1\ \text{ML}_{111}$ corresponds to $7.83 \times 10^{14}\ \text{atoms/cm}^2$. (Here, ML stands for monolayer.) The Ge/Si(111)- (5×5) structure is completed [29] at a coverage of $4\ \text{ML}_{111}$. In the following (if not differently stated), 1 ML refers to $1\ \text{ML}_{112}$, which is equal to $5.54 \times 10^{14}\ \text{cm}^{-2}$. Hence, $1\ \text{ML}_{112} = 1/\sqrt{2}\ \text{ML}_{111}$.

Results and discussion

In adsorption

A typical LEED pattern of the clean Si(112) surface with (111) and (5×5) facets is shown in **Figure 1(a)**. All spots line up in rows along the $[11\bar{1}]$ direction. Between the integer-order stripes, additional spots occur at $n/7$ and $n/2$ of the surface Brillouin zone (SBZ) along the $[1\bar{1}0]$ direction, as indicated by the red and green arrows, respectively. These fractional order spots can be assigned to a (7×7) reconstruction on the (111) facets and to a (2×1) reconstruction on the (5×5) facets [19].

Upon In adsorption, the faceted structure evolves via a disordered transition regime [a snapshot of this stage is shown in **Figure 1(b)**] into a flat surface with an ordered superstructure, as depicted in **Figure 1(c)**.

The dynamics of this transition is illustrated in **Figure 1(d)**. At the beginning of the deposition, the (00) spot becomes more intense, until it reaches its maximum at around 0.35 ML. This rise in intensity is explained in terms of surface smoothing. As the starting surface is completely decomposed into facets, there is no specular reflection along the $[112]$ surface normal direction at all, but the (00) signal plotted here is generated from rather diffuse intensity associated with the facet spots near the center of the LEED pattern. Smoothing of the surface will therefore very likely increase the specularly reflected intensity, as observed here. An even stronger evidence for surface smoothing is given by the evolution of the facet spot intensity, which drops more or less linearly with In coverage, until it reaches a constant level (which corresponds to diffuse background intensity only) at about 0.25 ML. Although the surface seems to be smooth at this stage, it is not very well ordered, as shown from the LEED pattern in **Figure 1(b)**. From this rather diffuse pattern, a clear indication for neither remnants of facets nor an ordered superstructure can be identified. When the indium deposit is further increased, the (00) intensity drops again. At the same time, new spots appear and become more intense, which we assign to an In-induced superstructure. As no change in the (00) intensity and in the superstructure spot intensities is observed after the exposure to around 0.8 ML, it is concluded that the newly formed structure is saturated at a coverage of about 0.8 ML. A typical LEED pattern recorded at the final stage is shown in **Figure 1(c)**. The yellow rectangle marks a reciprocal (1×1) unit mesh. The three spots labeled A_1 to A_3 and the three spots labeled B_1 to B_3 have the same spacing of about 28.5% SBZ for the preparation conditions used here. This finding could, in principle, be explained by the presence of a (7×1) structure, as proposed by Gai et al. [17]. However, these authors could not observe $(1/7\ n)$ or $(6/7\ n)$ superstructure spots. In addition, in our experiments, no electron energies could be found where these spots occur. This leads us to conclude that the average

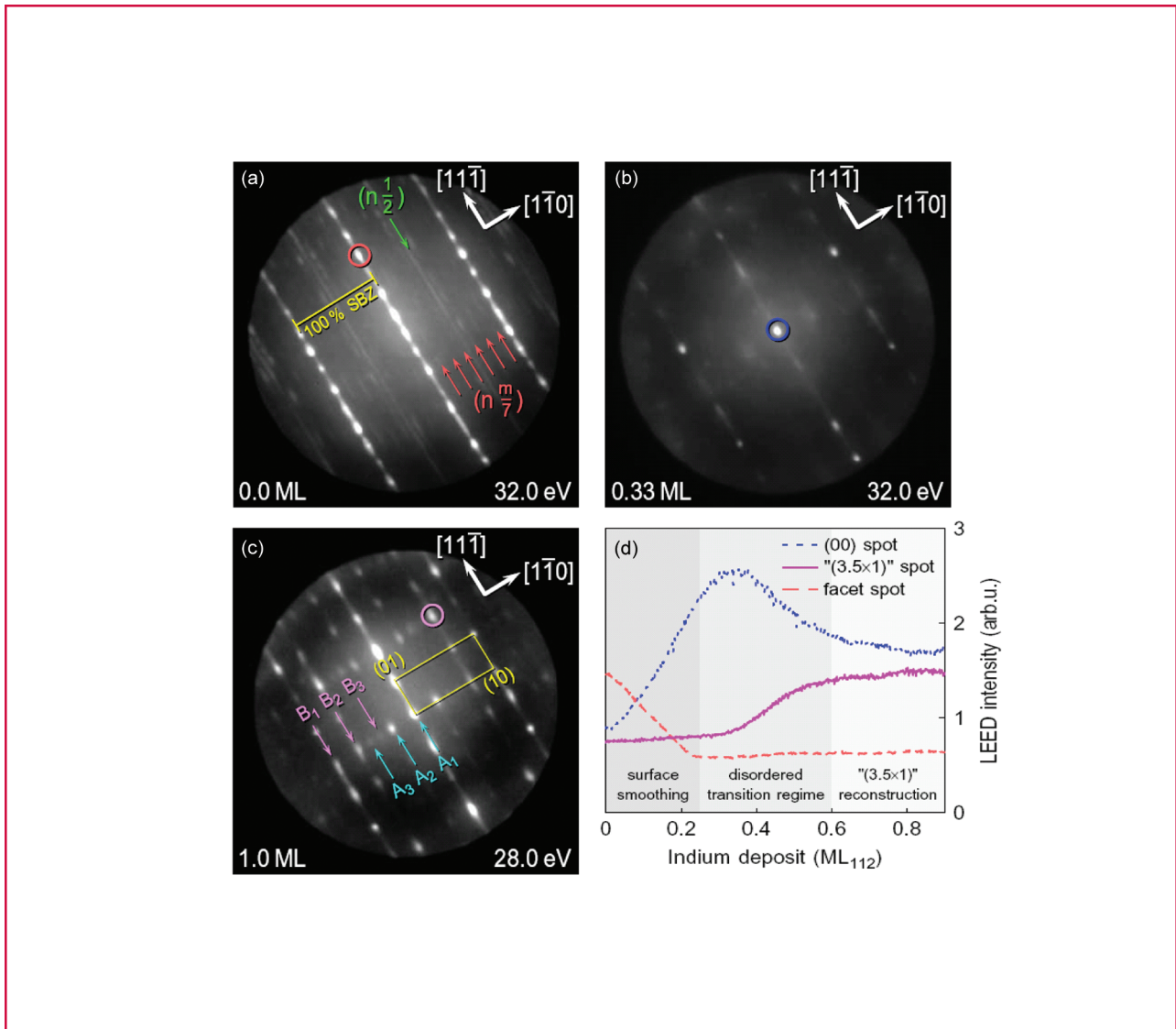


Figure 1

LEED patterns (a) prior, (b) during, and (c) after In deposition onto clean Si(112) at 500°C (logarithmic grayscale), as well as (d) evolution of the intensity of selected diffraction spots at 32 eV. The clean surface is composed of (111) and (5 × 12) facets, which expose (red arrows) a (7 × 7) reconstruction and (green arrow) a (2 × 1) reconstruction, respectively. In (c), the three spots labeled “A” and the three spots labeled “B” have the same spacing, leading to an average surface periodicity of [(3 + x) × 1]. The yellow rectangle shows the reciprocal (1 × 1) unit mesh. The spots whose intensities are plotted as a function of coverage in (d) are marked with circles in (a)–(c).

surface periodicity is indeed [(3 + x) × 1], with x = 0.5 in this case.

We assume that this “pseudoincommensurate” structure is composed of (3 × 1) and (4 × 1) building blocks, similar to the situation on the Ga/Si(112) surface. The latter mainly consists of (5 × 1) and (6 × 1) building blocks, as has been observed by scanning tunneling microscopy [20, 21], leading to a [(5 + x) × 1] LEED pattern [22]. Moreover, high-resolution LEED measurements (not shown here) prove that the value of x depends on the In coverage and

adsorption temperature, which clearly rules out a (7 × 1) reconstruction and is detailed elsewhere [30]. A common structural element in the (5 × 1) and (6 × 1) building blocks of the Ga/Si(112) surface are Ga vacancies that produce a missing-row structure. In one (6 × 1) building block, only 10 of the 12 possible Ga sites are occupied. Returning to the results for In/Si(112), and assuming a similar atomic configuration as for Ga/Si(112), i.e., including one or two In vacancies per building block, a saturation coverage between 0.67 and 0.875 ML is expected for a [(3 + x) × 1] periodicity,

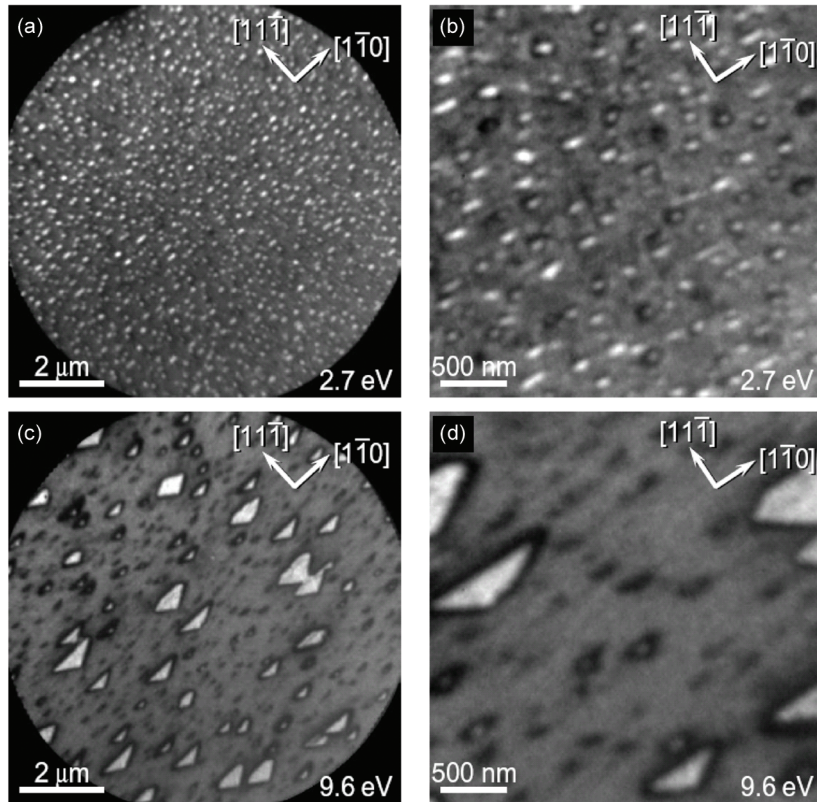


Figure 2

Bright-field LEEM images obtained after Ge growth on In-saturated Si(112) at [(a) and (b)] 450°C and [(c) and (d)] 500°C.

in agreement with our results. The similarity between the Ga/Si(112) and In/Si(112) atomic structures will be demonstrated by means of x-ray standing wave results in an upcoming publication [30].

Ge growth on In/Si(112)

As on the bare Si(112) surface [22], Ge growth on In-covered Si(112) leads to the formation of a wetting layer and, subsequently, to 3-D Ge islands. The island morphologies obtained for different growth temperatures are illustrated in the LEEM images in **Figure 2**. For growth at 450°C, as shown in Figure 2(a) and 2(b), essentially two island

geometries are found. In addition to islands with a rather isotropic appearance, Ge islands with a dashlike shape are also observed, extending along the $[1\bar{1}0]$ direction. The average size of the dashlike islands is estimated to be about 150 nm in the $[1\bar{1}0]$ direction and 70 nm in the $[11\bar{1}]$ direction. Most of the dashlike islands appear much brighter than the isotropic ones, whereas the latter tend to have a wider region with low LEEM intensity at their circumference. Since the LEEM contrast is influenced by form factors and field distortions, this finding might indicate that these two island types have different side facets that yield different intensities at the energy used here. Owing to the

small size of the islands and, thus, of their side facets, a detailed investigation of the facet orientations with LEED, as presented for the 500°C growth temperature below, was not possible in our experiments.

When the growth temperature is increased to 500°C, the surface morphology changes, as shown in Figure 2(c). Still, a few dashlike islands elongated in the $[1\bar{1}0]$ direction are observed, but most of the islands have a triangular outline, with the longest edge along $[1\bar{1}0]$ and with the apex pointing toward the $[\bar{1}\bar{1}1]$ direction. The size distribution of these triangular islands is rather broad. The vast majority of the Ge is incorporated into large islands, many of which approach or even exceed a width of 1 μm in $[1\bar{1}0]$ direction, as obvious from Figure 2(c). Nevertheless, there are also many triangular islands with a width below 350 nm, as shown in Figure 2(d).

Comparing the LEEM images for 450°C with those for 500°C, it is obvious that the island density decreases with increasing temperature. This is readily understood in terms of thermally activated diffusion. From a quantitative analysis of the dependence of the island density on growth temperature, the diffusion barrier height can be estimated within the framework of the classical nucleation theory [31], as has been demonstrated, e.g., in the case of Ge growth on bare and Ga-covered Si(112) and Si(113) surfaces [22, 32]. In the present case of Ge growth on In-terminated Si(112), unfortunately, only a very small temperature window was accessible in our experiments. When, on one hand, Ge was significantly grown below 450°C, the islands became too small and too dense for a reliable analysis. When, on the other hand, the growth temperature was raised well above 500°C, the desorption of In from the Ge wetting layer could no longer be compensated by In co-deposition. Hence, only a rough estimate of the diffusion barrier height can be given here. For 450°C, the island density is about $1.8 \times 10^9 \text{ cm}^{-2}$, which is comparable [22] with Ge growth on bare Si(112). At 500°C, however, the island density for Ge/In:Si(112) is nearly twice as high (about $3.6 \times 10^8 \text{ cm}^{-2}$) as for Ge/Si(112). Assuming an Arrhenius behavior for island density N , i.e., $N \propto \exp(E_A/k_B T)$, we obtain an activation energy E_A of approximately 1.5 eV, which is significantly smaller compared [22] with Ge/Si(112) ($E_A = 2.06 \text{ eV}$) and Ge/Ga/Si ($E_A = 2.35 \text{ eV}$). According to a previously detailed approximation [22, 32], a similarly reduced diffusion barrier is implied. Thus, in the presence of In on the Ge/Si(112) surface, the Ge adatom diffusion is enhanced. A similar impact of In adsorption on surface diffusion has been also reported for Ge/Si(111) [6].

A LEED pattern of the Ge/In:Si(112) surface after Ge growth at 500°C is shown in **Figure 3(a)**. It consists mainly of a $[(3+x) \times 1]$ pattern that is attributed to the In-terminated Ge wetting layer, which makes up the largest part of the surface. Within the experimental resolution, no change for the value of x is observed, as compared with the In:Si(112) starting surface. Hence, the periodicity (and,

presumably, the atomic structure) is virtually maintained upon Ge wetting layer formation.

Apart from the $[(3+x) \times 1]$ pattern, facet spots are visible, some of which have been marked by circles in Figure 3(a). When increasing the electron energy, these spots move toward the directions indicated by the arrows attached to the circles, whereas the $[(3+x) \times 1]$ spots are stationary on the projection screen. (Contrary to conventional LEED systems, where scattering angles are detected, the LEEM instrument probes the momentum transfer parallel to the surface. Thus, diffraction spots originating from flat regions on the surface appear at the same position for different energy levels.) Therefore, we attribute these additional spots to originate from Ge island side facets. The orientation of a facet can be determined from its azimuthal orientation, i.e., the projection of the facet's normal into the (112) surface plane, and the inclination of the facet normal direction with respect to the [112] surface normal direction. Both quantities can be determined from a series of LEED patterns as a function of electron energy. The azimuthal orientation is then identified by the direction into which the facet spots move, as indicated by the arrows in Figure 3(a). For the marked spots, we find three different azimuthal orientations, namely, $[11\bar{1}]$, $[\bar{7}\bar{1}4]$, and its symmetric counterpart $[\bar{1}\bar{7}4]$. This corresponds to the existence of three side facets, two of which are mirror symmetric with respect to the $[11\bar{1}]$ axis. The inclination angles have been determined from the reciprocal space maps (RSMs) shown in **Figure 3(c)** and **3(d)**. These RSMs were composed from line scans through the stack of LEED patterns for different energy levels. In particular, for low energies, the $K_{\parallel}-K_{\perp}$ dependence within a single LEED pattern becomes important. This dependence has been accounted for, which leads to the curved contours of the RSMs. The RSM shown in Figure 3(c) was taken along the $[11\bar{1}]$ direction through the (00) spot. Therefore, all the $(0n)$ spots appear as vertical reciprocal lattice rods in this RSM. Apart from these vertical rods, at least two inclined rods can be identified, which are marked by arrows in Figure 3(c). These oblique rods are tilted toward the $[11\bar{1}]$ direction by 20.3°, which is in reasonable agreement with the inclination of 19.5° expected for a (111) facet. In Figure 3(d), an RSM taken along the $[\bar{7}\bar{1}4]$ direction through the $(0\bar{1})$ spot is shown. Again, some vertical rods appear, which originate from the $(0\bar{1})$ spot in the center and the (31) and $(\bar{3}\bar{1})$ spots near the edge of the RSM. Some other weak vertical rods appear in between, which are attributed to $[(3+x) \times 1]$ superstructure spots that are close to the plane of the RSM. In addition, one inclined rod marked by arrows is clearly visible. Its tilt angle of 24.6° toward the $[\bar{7}\bar{1}4]$ direction agrees well with the angle of 25.4° expected for a (013) facet. Its symmetric counterpart, then, is a (103) facet. Although there are indications for additional oblique rods in both Figures 3(c) and 3(d), none of these is sufficiently intense to unambiguously be identified. Therefore, we conclude that the

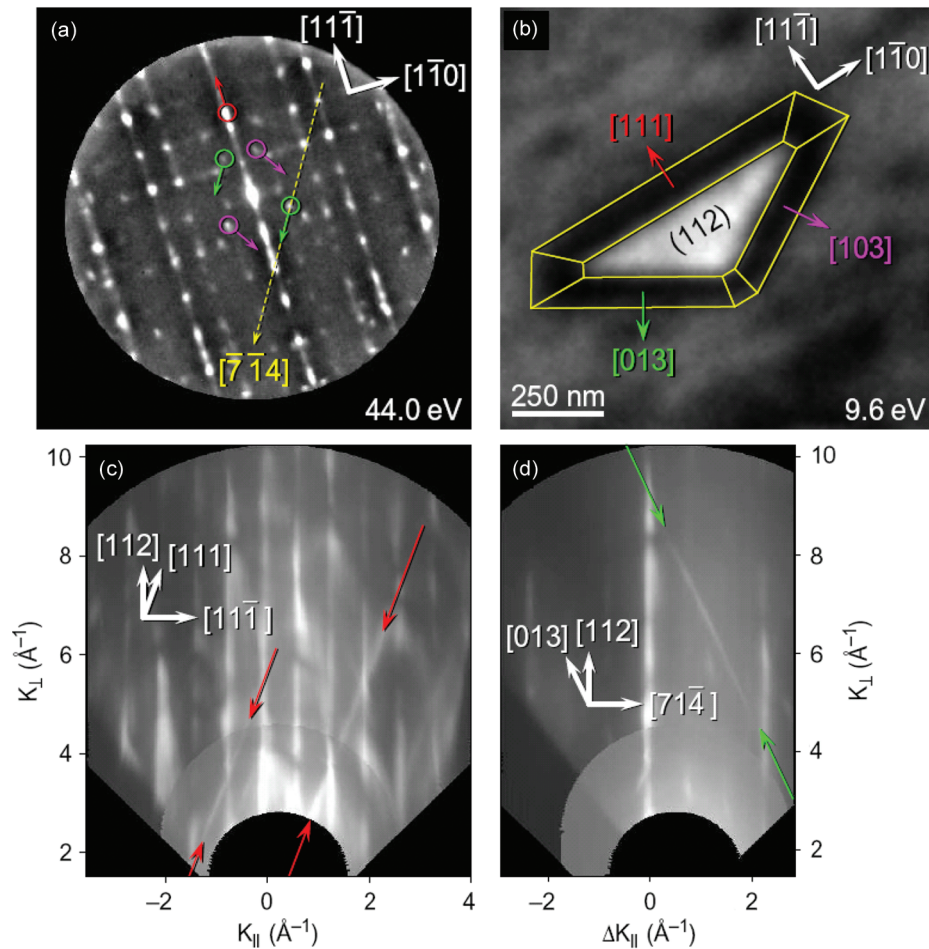


Figure 3

LEED and LEEM patterns. (a) LEED pattern (logarithmic grayscale), (b) bright-field LEEM image of an island, and (c) and (d) reciprocal space maps (RSMs) for Ge grown on In-terminated Si(112) at 500°C. In (a), several facet spots have been marked with circles. The arrows indicate into which direction the facet spots move with increasing electron energy. The RSMs were taken (c) through the (00) spot along the $[11\bar{1}]$ direction and (d) through the $(0\bar{1})$ spot along the $[7\bar{1}4]$ direction. The reciprocal lattice rods related to (111) and (013) facets are marked with arrows in (c) and (d), respectively. The LEED pattern in (a) has been high-pass filtered to make the facet spots better visible.

Ge islands are mainly terminated by (111) and {103} side facets. A real-space image of a typical Ge island is shown in **Figure 3(b)**, where the facet geometry is superimposed. The

top (112) facet appears bright, whereas all side facets are dark. This is in agreement with geometrical LEED simulations (not shown here), which imply that, at the

electron energy used here, neither the (111) nor the {103} facets contribute to the (00) intensity and, thus, to the bright-field LEEM intensity.

Note added in proof: The In-terminated {103} facets observed here have most likely a (1×1) reconstruction [33], as this type of facet has been shown to be energetically very favorable in theoretical work [34], and such facets are also found after In adsorption on bulk Ge(001) [35] and bulk Ge(113) [36].

Conclusion

The adsorption of In on Si(112) and its influence on the surface morphology and atomic structure, as well as its impact on subsequent Ge growth, has been studied with LEEM and LEED.

The initially faceted Si(112) is smoothed upon In adsorption, and a complex superstructure is formed. In contrast to a previously proposed (7×1) structure [17], our results indicate the existence of a “pseudoincommensurate” $[(3+x) \times 1]$ structure that consists of (3×1) and (4×1) building blocks, similar to Ga/Si(112), where a $[(5+x) \times 1]$ is reported [22] that consists of (5×1) and (6×1) unit cells [20, 21]. The In:Si(112)- $[(3+x) \times 1]$ structure saturates at a coverage of around 0.8 ML, which agrees with a vacancy “pseudoincommensurate” model.

For subsequent Ge growth, a strong influence of In preadsorption on the island morphology has been found. Whereas on bare Si(112), islands with a rather circular outline have been reported [22], anisotropic islands are observed in the presence of In, the shape, size, and density of which depend on growth temperature. At 450°C, dashlike islands are formed, whereas at 500°C, mainly triangular islands occur, the side facets of which have been determined to be of (111) and {103} orientations.

Acknowledgments

The authors would like to thank P. Sutter, J. T. Sadowski, and P. Zahl for technical support at Brookhaven National Laboratory. This work was supported in part by the Deutsche Forschungsgemeinschaft under Grant FA 363/6 and in part by the Physics International Postgraduate Program of the University of Bremen (supported by the German Academic Exchange Service). The experiments were carried out in whole at the Center for Functional Nanomaterials, Brookhaven National Laboratory, which is supported by the Division of Materials Sciences and Division of Chemical Sciences, U.S. Department of Energy, under Contract DE-AC02-98CH10886.

References

1. M. Copel, M. C. Reuter, E. Kaxiras, and R. M. Tromp, “Surfactants in epitaxial growth,” *Phys. Rev. Lett.*, vol. 63, no. 6, pp. 632–635, Aug. 1989.
2. F. K. LeGoues, M. Copel, and R. M. Tromp, “Microstructure and strain relief of Ge films grown layer by layer on Si(001),”

- Phys. Rev. B*, vol. 42, no. 18, pp. 11 690–11 700, Dec. 1990.
3. M. Horn-von Hoegen, F. K. LeGoues, M. Copel, M. C. Reuter, and R. M. Tromp, “Defect self-annihilation in surfactant-mediated epitaxial growth,” *Phys. Rev. Lett.*, vol. 67, no. 9, pp. 1130–1133, Aug. 1991.
4. H. Nakahara and M. Ichikawa, “Molecular beam epitaxial growth of Si on Ga-activated Si(111) surface,” *Appl. Phys. Lett.*, vol. 61, no. 13, pp. 1531–1533, Sep. 1992.
5. J. Falta, M. Copel, F. K. LeGoues, and R. M. Tromp, “Surfactant coverage and epitaxy of Ge on Ga-terminated Si(111),” *Appl. Phys. Lett.*, vol. 62, no. 23, pp. 2962–2964, Jun. 1993.
6. B. Voigtländer, A. Zinner, T. Weber, and H. P. Bonzel, “Modification of growth kinetics in surfactant-mediated epitaxy,” *Phys. Rev. B*, vol. 51, no. 12, pp. 7583–7591, Mar. 1995.
7. H. Minoda, S. Sakamoto, and K. Yagi, “*In situ* REM observations of surfactant-mediated epitaxy: Growth of Ge on Si(111) surfaces mediated by Bi,” *Surf. Sci.*, vol. 372, no. 1–3, pp. 1–8, Feb. 1997.
8. Th. Schmidt, R. Kröger, T. Clausen, J. Falta, A. Janzen, M. Kammiller, P. Kury, P. Zahl, and M. Horn-von Hoegen, “Surfactant-mediated epitaxy of Ge on Si(111): Beyond the surface,” *Appl. Phys. Lett.*, vol. 86, no. 11, pp. 111910-1–111910-3, Mar. 2005.
9. T. F. Wietler, E. Bugiel, and K. R. Hofmann, “Relaxed germanium films on silicon(110),” *Thin Solid Films*, vol. 517, no. 1, pp. 272–274, Nov. 2008.
10. K. Schroeder, A. Antons, R. Berger, and S. Blügel, “Surfactant mediated heteroepitaxy versus homoepitaxy: Kinetics for group-IV adatoms on As-passivated Si(111) and Ge(111),” *Phys. Rev. Lett.*, vol. 88, no. 4, article no. 046101, Jan. 2002.
11. Th. Schmidt, J. I. Flege, S. Gangopadhyay, T. Clausen, A. Locatelli, S. Heun, and J. Falta, “Alignment of Ge nanoislands on Si(111) by Ga-induced substrate self-patterning,” *Phys. Rev. Lett.*, vol. 98, no. 6, article no. 066104, Feb. 2007.
12. H. Omi and T. Ogino, “Self-organization of Ge islands on high-index Si substrates,” *Phys. Rev. B*, vol. 59, no. 11, pp. 7521–7528, Mar. 1999.
13. J.-H. Zhu, K. Brunner, G. Abstreiter, O. Kienzle, F. Ernst, and M. Rühle, “Correlated SiGe wires shaped by regular step bunches on miscut Si(113) substrates,” *Phys. Rev. B*, vol. 60, no. 15, pp. 10 935–10 940, Oct. 1999.
14. Th. Schmidt, T. Clausen, J. I. Flege, S. Gangopadhyay, A. Locatelli, T. O. Mentes, F. Z. Guo, S. Heun, and J. Falta, “Adsorbate induced self-ordering of germanium nanoislands on Si(113),” *New J. Phys.*, vol. 9, p. 392, Oct. 2007.
15. E. Kaxiras, “Interplay of strain and chemical bonding in surfactant monolayers,” *Europhys. Lett.*, vol. 21, no. 6, pp. 685–690, Feb. 1993.
16. J. Falta, Th. Schmidt, A. Hille, and G. Materlik, “Surfactant adsorption site and growth mechanism of Ge- on Ga-terminated Si(111),” *Phys. Rev. B*, vol. 54, no. 24, pp. R17 288–R17 291, Dec. 1996.
17. Z. Gai, R. G. Zhao, W. S. Yang, and T. Sakurai, “Atomic structure of the Si(112) 7×1 -In surface,” *Phys. Rev. B*, vol. 61, no. 15, pp. 9928–9931, Apr. 2000.
18. A. A. Baski and L. J. Whitman, “A scanning tunneling microscopy study of hydrogen adsorption on Si(112),” *J. Vac. Sci. Technol. A, Vac. Surf. Films*, vol. 13, no. 3, pp. 1469–1472, May 1995.
19. A. A. Baski, S. C. Erwin, and L. J. Whitman, “The structure of silicon surfaces from (001) to (111),” *Surf. Sci.*, vol. 392, no. 1–3, pp. 69–85, Dec. 1997.
20. C. González, P. C. Snijders, J. Ortega, R. Pérez, F. Flores, S. Rogge, and H. H. Weitering, “Formation of atom wires on vicinal silicon,” *Phys. Rev. Lett.*, vol. 93, no. 12, article no. 126106, p. 4, Sep. 2004.
21. P. C. Snijders, S. Rogge, C. González, R. Pérez, J. Ortega, F. Flores, and H. H. Weitering, “Ga-induced atom wire formation and passivation of stepped Si(112),” *Phys. Rev. B*, vol. 72, no. 12, article no. 125343, Sep. 2005.
22. M. Speckmann, Th. Schmidt, J. I. Flege, J. T. Sadowski, P. Sutter, and J. Falta, “Temperature dependent low-energy electron microscopy study of Ge island growth on bare and Ga terminated

- Si(112),” *J. Phys., Condens. Matter.*, vol. 21, no. 31, article no. 314020, Jul. 2009.
23. J. I. Flege, E. Vescovo, G. Nintzel, L. H. Lewis, S. Hulbert, and P. Sutter, “A new soft X-ray photoemission microscopy beamline at the National Synchrotron Light Source,” *Nucl. Instr. Meth. Phys. Res. B*, vol. 261, no. 1/2, pp. 855–858, Aug. 2007.
 24. H. Hibino and T. Ogino, “Exchanges between group-III (B, Al, Ga, In) and Si atoms on Si(111)- $\sqrt{3} \times \sqrt{3}$ surfaces,” *Phys. Rev. B*, vol. 54, no. 8, pp. 5763–5768, Aug. 1996.
 25. J. Nogami, S.-i. Park, and C. F. Quate, “Indium-induced reconstructions of the Si(111) surface studied by scanning tunneling microscopy,” *Phys. Rev. B*, vol. 36, no. 11, pp. 6221–6224, Oct. 1987.
 26. J. Kraft, M. G. Ramsey, and F. P. Netzer, “Surface reconstructions of In on Si(111),” *Phys. Rev. B*, vol. 55, no. 8, pp. 5384–5393, Feb. 1997.
 27. N. Nakamura, K. Anno, and S. Kono, “Structure analysis of the single-domain Si(111) 4×1 -In surface by μ -probe Auger electron diffraction and μ -probe reflection high energy electron diffraction,” *Surf. Sci.*, vol. 256, no. 1/2, pp. 129–134, Oct. 1991.
 28. J. Wang, H. Wu, R. So, Y. Liu, M. H. Xie, and S. Y. Tong, “Structure determination of indium-induced Si(111)-In- 4×1 surface by LEED Patterson inversion,” *Phys. Rev. B*, vol. 72, no. 24, article no. 245324, Dec. 2005.
 29. U. Köhler, O. Jusko, G. Pietsch, B. Müller, and M. Henzler, “Strained-layer growth and islanding of germanium on Si(111)-(7×7) studied with STM,” *Surf. Sci.*, vol. 248, no. 3, pp. 321–331, Jun. 1991.
 30. M. Speckmann, Th. Schmidt, J. I. Flege, J. Höcker, I. Heidmann, and J. Falta, *Ga- and In-induced reconstructions of the Si(112) surface*, 2011, in preparation.
 31. J. A. Venables, G. D. T. Spiller, and M. Hanbücken, “Nucleation and growth of thin films,” *Rep. Prog. Phys.*, vol. 47, no. 4, pp. 399–459, Apr. 1984.
 32. T. Clausen, Th. Schmidt, J. I. Flege, A. Locatelli, T. O. Menten, S. Heun, F. Z. Guo, and J. Falta, “Temperature-dependent low-energy electron microscopy study of Ge growth on Si(113),” *Appl. Surf. Sci.*, vol. 252, no. 15, pp. 5321–5325, May 2006.
 33. O. Bunk, G. Falkenberg, J. H. Zeysing, L. Lottermoser, R. L. Johnson, M. Nielsen, F. Berg-Rasmussen, and R. Feidenhans’l, “Structure determination of the indium-induced Ge(103)- 1×1 reconstruction by surface X-ray diffraction,” *Appl. Surf. Sci.*, vol. 142, no. 1-4, pp. 88–93, Apr. 1999.
 34. F.-C. Chuang, “First-principles study of indium-stabilized {103} facets in Ge quantum dots,” *Phys. Rev. B*, vol. 75, no. 11, article no. 115408, Mar. 2007.
 35. M. Nielsen, D.-M. Smilgies, R. Feidenhans’l, E. Landemark, G. Falkenberg, L. Lottermoser, L. Seehofer, and R. L. Johnson, “Hut clusters on Ge(001) surfaces studied by STM and synchrotron X-ray diffraction,” *Surf. Sci.*, vol. 352–354, pp. 430–434, May 1996.
 36. H. Ji, R. G. Zhao, and W. S. Yang, “Surface reconstruction and faceting of group III/IV(113) systems—Common characteristics of the stable surface structures,” *Surf. Sci.*, vol. 371, no. 2/3, pp. 349–357, Feb. 1997.

Received September 30, 2010; accepted for publication April 5, 2011

Moritz Speckmann *Institute of Solid State Physics, University of Bremen, Otto-Hahn-Allee 1, 28 359 Bremen, Germany (mspeckmann@ifp.uni-bremen.de).*

Thomas Schmidt *Institute of Solid State Physics, University of Bremen, Otto-Hahn-Allee 1, 28 359 Bremen, Germany (tschmidt@ifp.uni-bremen.de).*

Jan Ingo Flege *Institute of Solid State Physics, University of Bremen, Otto-Hahn-Allee 1, 28 359 Bremen, Germany (flege@ifp.uni-bremen.de).*

Jens Falta *Institute of Solid State Physics, University of Bremen, Otto-Hahn-Allee 1, 28 359 Bremen, Germany (falta@ifp.uni-bremen.de).*